A. BHATTACHARYA
Research Assistant.

J. H. LIENHARD
Professor. Mem. ASME

Department of Mechanical Engineering,
University of Kentucky,
Lexington, Ky.

Hydrodynamic Transition in Electrolysis[1]

The gas removal process during electrolysis is studied with the aim of identifying hydrodynamic transitions, analogous to those which occur in boiling. The local peak in the electrolysis gas flux is observed during electrolysis from a horizontal cylindrical cathode. This transition point is shown to correspond with Moissis and Berenson's "first transition" in nucleate pool boiling. A prediction of the transition, applicable to either boiling or electrolysis, is developed for the cylindrical heater (or cathode) arrangement. It is compared with 12 experimental data for boiling and electrolysis, and its limitations are discussed. Finally, some attributes of the regime of film electrolysis are identified and discussed.

Introduction

ELECTROLYSIS has attracted increasing interest lately because of its relevance to a variety of problems of human life support and a myriad of industrial processes. References [1, 2][2] provide some background as to the scope of contemporary applications of electrolysis. The present study is part of a broad effort to establish the similarity between boiling and electrolysis. We have generally sought to establish means for applying known methods for predicting boiling processes to the prediction of comparable processes in electrolysis. In [3] we dealt with bubble growth predictions for the two processes, and here we look for hydrodynamic transitions comparable to those which occur during boiling.

Fig. 1 is a conventional boiling curve with a transformed ordinate. In it, the vapor volume flux v (or the heat flux q divided by the volumetric latent heat of vaporization, $\rho_g h_{fg}$) is plotted against the driving temperature difference ΔT. The well-known transitions in the boiling mechanisms are indicated on this figure. Let us consider each one briefly.

1 Inception. This is the point at which the first bubbles appear. Since we are not concerned with predicting inception in either boiling or electrolysis, we shall make no attempt here to recount the massive literature on the subject.

2 Transition From the Isolated Bubble Region to the Region of Slugs and Columns. This transition was identified by Zuber [4, 5]. It was subsequently predicted by Moissis and Berenson [6], who also advanced a variety of measurements of the transition point.

Using observations of the rise of bubbles in tubes [7, 8] Moissis and Berenson showed that the volume flux at this transition, v_{sc}, can be given as[3]

[3] Symbols not explained in context are ones in common use. They are defined in the Nomenclature.

Nomenclature

A = area of cathode or of a heating element

A_g = area of escaping gas or vapor jets

C_1 = constant in $v_{\min_F}$ expression, equation (8)

C_2 = constant in $v_{\min_{cyl}}$ expression, equation (10)

C_3 = fraction of axial distance, on cathode or heating element, occupied by gas or vapor jets

D_b = bubble diameter at departure from cathode or heating element

E = voltage drop between cathode and anode

E_{c-b} = voltage drop from cathode to nearby liquid bulk

g = acceleration of gravity

h_{fg} = latent heat of vaporization

I = electrical current

L = spacing between adjacent vapor jets

M = molecular weight (of hydrogen in the present case)

n = nucleation site density, or number of electrons (2) per H_2 atom formed by electrolysis

q = heat flux

R = radius of cathode or heating element

(Continued on next page)

1
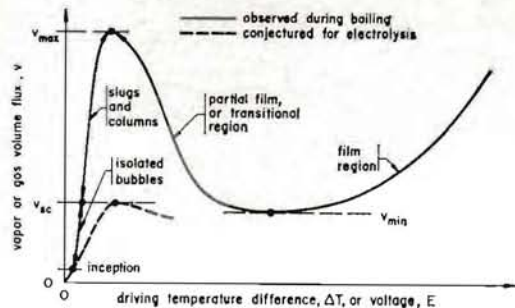
Fig. 1 Schematic boiling curve and corresponding conjectured electrolysis curve

$$v_{\mathrm{sc}} = 0.56\beta^{1/2} \sqrt[4]{g\sigma/(\rho_f - \rho_g)} \, \frac{A_g}{A} \tag{1}$$

where β is the contact angle of the liquid-vapor interface on the heater, and A_g/A is the fraction of the heater area occupied by vapor jets. Zuber [9] argued that the vapor jet pattern—once set up—is constant and the velocity of vapor flow through these jets increases with q or v. He further argued that the jets form an array spaced on a square grid and that they have a diameter of half the grid size. This gave $A_g/A = \pi/16$ for a flat plate, so

$$v_{\mathrm{sc}} = 0.11\beta^{1/2} \sqrt[4]{g\sigma/(\rho_f - \rho_g)} \tag{2}$$

In the published discussion of [6], both Chang and Zuber asked the authors if this transition was well defined. They replied that it was indeed slurred so that equation (2) is an approximate result. We shall return to this point later.

3 The Peak Volume Flux Transition. Zuber [9, 10] originally predicted v_{max} for boiling on horizontal flat plates. He noted that the velocity of escaping vapor in the jets eventually causes the jets to become Helmholtz unstable and the efficient process of vapor removal by jetting collapses. The spacing of the grid on which the jets are placed is equal to the most rapidly collapsing Taylor unstable wavelength, λ_d, in the liquid-over-vapor interface above the plate. This wavelength was shown by Bellman and Pennington [11] to be

$$\lambda_d = 2\pi\sqrt{3} \sqrt{\sigma/g(\rho_f - \rho_g)} \tag{3}$$

The maximum vapor volume flux obtained by Zuber as the analytical result of this description[4] was

---

[4] This result, along with most of the results we shall present here, is valid for $\rho_f/\rho_g \gg 1$—that is, up to system pressures within about 90 percent of the critical pressure.

$$v_{\mathrm{max}_F} = \frac{\pi}{24} \sqrt[4]{g\sigma(\rho_f - \rho_g)/\rho_g{}^2} \tag{4}$$

This expression compared well with data for flat plates.

Sun and Lienhard [12] subsequently made a similar prediction for horizontal cylindrical heaters. They obtained, for $R' > 0.15$,

$$v_{\mathrm{max}_{\mathrm{cyl}}} = v_{\mathrm{max}_F} \, (0.89 + 2.27 \exp\,[-3.44R'^{1/2}]) \tag{5}$$

where R' is a dimensionless radius defined as

$$R' \equiv \frac{2\pi\sqrt{3}R}{\lambda_d} = R \sqrt{g(\rho_f - \rho_g)/\sigma} \tag{6}$$

Ded and Lienhard [13] recently developed the corresponding expression for spheres. It is

$$v_{\mathrm{max}_{\mathrm{sph}}} = \begin{cases} 1.74R'^{-1/2} v_{\mathrm{max}_F}, & R' < 4.26 \\ 0.84 v_{\mathrm{max}_F}, & R' > 4.26 \end{cases} \tag{7}$$

Equations (5) and (7) were verified by a great deal of experimental data.

4 The Minimum Heat Flux Transition. Zuber also predicted v_{min} by considering a grid of waves in the liquid-vapor interface over a flat plate. The waves, spaced on a $\lambda_d \times \lambda_d$ grid, collapse cyclically to release bubbles of diameter $\lambda_d/2$ at the nodes. When the volume flux falls below that required to move the interface at its natural frequency, film boiling collapses. Zuber's analysis of this process [7, 8] yielded

$$v_{\mathrm{min}_F} = C_1 \sqrt[4]{\sigma g \, \frac{\rho_f - \rho_g}{(\rho_f + \rho_g)^2}} \tag{8}$$

where C_1 was predicted to be 0.177. Berenson [14] subsequently showed that Zuber's evaluation of C_1 involved an incorrect averaging and that it should actually be evaluated empirically. He found that $C_1 = 0.09$ gave good correlation with data.

Lienhard and Wong [15] subsequently modified this development for horizontal cylinders. They corrected λ_d for transverse curvature and obtained

$$\lambda_{d_{\mathrm{cyl}}} = \lambda_d \sqrt{\frac{1}{1 + 0.5R'^{-2}}} \tag{9}$$

The minimum volume flux for cylinders, based upon this wavelength, was found to be

$$v_{\mathrm{min}_{\mathrm{cyl}}} = v_{\mathrm{min}_F} \left[\frac{C_2}{R'^2(2R'^2 + 1)} \right]^{1/4} \tag{10}$$

where C_2 was found experimentally to be 1.289.

There is a general failing to these v_{min} expressions that does not afflict v_{max}. Berenson showed that while v_{max} is insensitive to surface condition, v_{min} can be strongly influenced by minor

---

Nomenclature

R' = dimensionless radius, $R\sqrt{g(\rho_f - \rho_g)/\sigma}$

v = volume flux from cathode or heating element

$v_{\mathrm{max}}, \atop v_{\mathrm{min}}, v_{\mathrm{sc}}$ = volume flux at the "second" (or Helmholtz unstable) transition, at the minimum film electrolysis or boiling transition, and at the "first" (or isolated-bubbles to slugs-and-columns) transition, respectively

β = contact angle or angle between liquid-vapor (or gas) interface and heater (or cathode) surface, measured on the liquid side

ΔT = temperature difference between a heating element and the saturated liquid adjacent to it

λ_d = most "dangerous" or most susceptible wavelength in a horizontal liquid-vapor interface, $2\pi\sqrt{3}$ $\left(\sqrt{\sigma/g(\rho_f - \rho_g)}\right)$

ρ_f = density of saturated liquid or of electrolyte

ρ_g = density of saturated vapor or of gas generated at cathode

ρ_{H_2} = density of gaseous hydrogen (special case for ρ_g)

σ = surface tension

F = subscript denoting infinite flat plate

cyl = subscript denoting horizontal cylinder

sph = subscript denoting sphere

variations of surface condition. Kovalev [16] further amplified the point and showed that the end-mounting of cylinders also influenced $v_{min_{cyl}}$. On the basis of Kovalev's data, Lienhard [17] showed that C_2 should be further reduced to at least 0.0217—perhaps even further. Thus v_{min} predictions are generally a chancey business. What the real minimum is, cannot finally be predicted, and it is very hard to ascertain experimentally.

Transitions in Electrolysis

At first glance we should expect the same transitions to exist in the volume flux *versus* voltage curve for electrolysis, as exist in the boiling curve, Fig. 1. While v is equal to $q/\rho_g h_{fg}$ in boiling, it can be obtained from Faraday's law for electrolysis. Faraday's law expresses the mass flux of H_2 dissociated at the cathode as proportional to the current flux, I/A amps per unit area, the molecular weight of H_2, and n^{-1} where n is the number of electrons transferred in the liberation of one H_2 molecule (for H_2, n, and M both equal 2). Thus

$$v = \frac{(I/A)M}{96500\, \rho_{H_2} n} \quad \frac{cm^3}{cm^2\, sec} \tag{11}$$

and we can reduce the current to a volume flux just as we could q.

Let us now consider a basic difference between nucleate boiling and nucleate electrolysis. The basic mechanism of heat removal in nucleate boiling was shown by Zuber [4, 5] to be microconvection driven by the rising bubbles. In 1962 Tien [18] predicted the microconvective heat flux in the region of isolated bubbles using an inverted stagnation flow model. Boehm and Lienhard [19] summarized and extended this type of prediction in 1964 and found that in the region of isolated bubbles

$$q \sim v \sim \Delta T^{1.18} n^{1/2} \tag{12}$$

where the "site density," n, is the number of nucleation sites per unit area.

During nucleate boiling, the site density typically rises as ΔT^6 or more. Thus q or v typically rises as $\Delta T^{3\ \text{or}\ 4}$. But during electrolysis there should be no corresponding convective enhancement of charge removal. The diffusion coefficient for H_2 created at the wall is very small (about 1/30 of the thermal diffusivity of the water). Thus the Schmidt number is on the order of 100 and the diffusion boundary layer is very much thinner than the microconvective velocity boundary layer. Furthermore, we find a heavy density of idle bubbles scattered in among the active or repeating sites during electrolysis. These create a static sublayer of fluid whose thickness is independent of the microconvective velocity, and which should totally contain the diffusion layer. Thus v should simply increase in direct proportion to the driving voltage, E. None of the convective reinforcement by the nucleation sites, which occurs in boiling, is present. In electrolysis it is as though the sites were not there, insofar as the relation between v and E is concerned.

An important aspect of the transition from the region of isolated bubbles to the region of slugs and columns is the blanketing-over, and removal of liquid-metal contact that occurs. Throughout the isolated bubble region there is virtually no loss of contact, but as the slugs and columns evolve, there is. Zuber [5], in fact, envisioned that this loss of contact increases, honeycombing the liquid under the jets and feeding them. This can continue until *more* than $\pi/16$ of the contact is eliminated and large dry patches cover the heater (see, e.g., the photographs of Kirby and Westwater [20] which dramatically show this behavior).

The heat transfer continues to increase strongly with ΔT in the region of slugs and columns because as the vapor velocity increases and heater surface is exposed, the microconvection at the surface continues to improve. Quite the opposite should occur during electrolysis, however. As contact is lost, the electric
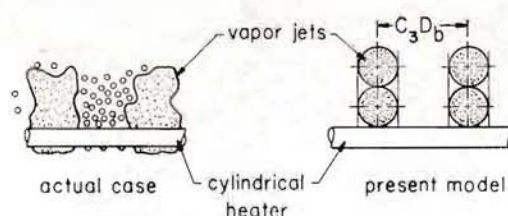
Fig. 2 Vapor removal pattern on horizontal cylinders at the "first-transition" point

current—and with it, v—must decrease in the absence of a convective process.

We are interested, then, in learning to predict the hydrodynamic transition from the region of isolated bubbles to the region of slugs and columns, or the "first transition" as we shall call it. This transition should replace the Helmholtz unstable transition as the point of peak volume flux, in electrolysis. It can be predicted for electrolysis on a flat plate with the help of equation (2). Since the experimental work presented here is done on horizontal wires, it will next be necessary to develop an equivalent expression for cylindrical cathodes.

On a cylindrical element, A_g/A must be modified for use with equation (1). On small wires, the bubbles rise from the wire, as indicated in Fig. 2, eventually following one another without interruption in a column of diameter, D_b, equal to that of the departing bubbles.[5] In this case

$$\frac{A_g}{A} = \frac{(\pi/4)D_b^2}{2\pi RL} = \frac{D_b}{8C_3 R} \tag{13}$$

where L, the length of wire subtended by one column, is equal to $C_3 D_b$. The constant $1/C_3$ is the fraction of the wire's length occupied by columns. In Moissis and Berenson's model, C_3 would be equal to 2, measured along the rectangular grid lines, and equal to $2\sqrt{2}$ or 2.83 on diagonal lines through the grid. The spacing should be comparable for cylinders, but we have no way of specifying the precise value of C_3 a priori.

Using Fritz's [21] expression for the bubble departure diameter, D_b,

$$D_b = 0.0148\beta \sqrt{\frac{2\sigma}{g(\rho_f - \rho_g)}} \tag{14}$$

in equation (13), and then substituting equation (13) in equation (1) we obtain

$$v_{se} = \frac{0.001464}{C_3} \frac{\beta^{1/2}}{R'} \sqrt[4]{\frac{g\sigma}{\rho_f - \rho_g}} \tag{15}$$

for the volume flux at the first transition on small cylinders. Sun's [12] experiments with boiling show that the transition from small to large cylinder behavior occurs above $R' = 3$. We expect that equation (15) will probably apply up to a comparable value of R'.

Experiments

A local maximum in electrolytic gas evolution has been observed in the past. In 1950, for example, Kellogg [22] reported observations of such a maximum during aqueous electrolysis from a vertical wire anode. Actually this transition was known then in connection with the "anode-effect," or the vapor blanketing of anodes which had been observed much earlier during the electrolysis of molten salts. The concern in this case was not with predicting (or even explaining) the peak but with identifying the phenomenon of film electrolysis and, noting that it resulted in a considerable reduction of current at a given voltage. One

_____
[5] This conceptualization is consistent with that of Moissis and Berenson for flat plates.

3
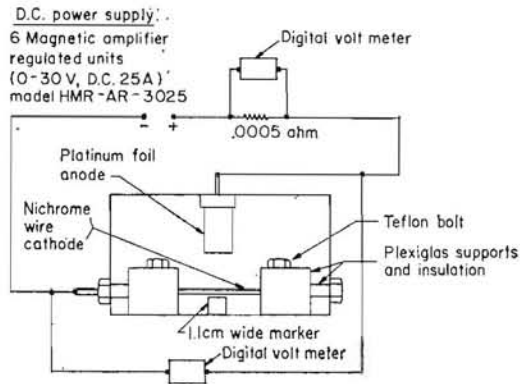
Fig. 3 Test capsule and the circuit diagram for the electrolysis experiment

Fig. 4 Variation of volume flux with voltage during electrolysis

Fig. 5 Comparison of $I(E)$ and $I(E_{c-b})$ on logarithmic coordinates

important *en passent* observation made by Kellogg was that "the current increases almost linearly with increased voltage" in the region approaching the local maximum. This concurs with the result we anticipated in the previous section.

Two basic experiments have been undertaken in the present study to test our predictions as to the nature of the electrolysis curve. In one of the tests we measured the I (or V) versus E curve during electrolysis from cylinders, and obtained photographic verification of aspects of the process. In the other we measured v_{sc} during boiling to provide additional corroboration of equation (15).

Fig. 3 shows the apparatus for the electrolysis experiment. A one-tenth normal KOH electrolyte was contained in a 3.45 in. $\times$ 4 in. $\times$ 7.5 in. plexiglas box. Clean nichrome wire cathodes (14, 16, and 20 gauge and about 2 in. in length) were suspended in the electrolyte. The anode was made of clean platinum foil and suspended in the electrolyte above the cylinder. It was made considerably larger in surface area than the cathode to assure that it would function in the isolated bubble regime long after the cathode underwent any transition. Additional details relating to the experiment are given by Bhattacharya [24].

Fig. 4 shows the basic output of the experiment for three of the wire sizes (14, 16, and 20 gauge). These v versus E curves were obtained by increasing the voltage across the test cell up to the desired value, stabilizing the temperature within a 15 deg F range, and measuring the current, I. Equation (11) was then used to calculate v from I. It was necessary to operate in a fairly high temperature range because, at high currents, the capsule heated up rapidly during the course of an observation. We were generally able to hold temperatures close to 160 deg F when the potential was below about 100 volts; but it was increasingly hard to do so when we had to increase the voltage through the region of peak current before making an observation.

The curves were quite regular and reproducible up to a maximum value of v. Beyond this maximum, the data exhibited a great deal of scatter and indeed the current was unsteady and tended to fluctuate at a given voltage. Nevertheless the current clearly dropped off dramatically with voltage beyond the peak. At the maximum volume flux a blue corona first formed in the vapor separating the cathode from the liquid. As the voltage was further increased the corona also increased, and with it there developed intermittent sparking between the cathode and the electrolyte. As we approached our maximum voltage capability of about 180 volts, the sparking assumed a regular spacing and fairly great intensity.

We should emphasize that the abscissa in Fig. 4 (the voltage between the cathode and the anode) is only *proportional* to—not equal to—the driving voltage of the surface electrolysis process. This fact was clarified by a duplicate run on a 16-gage wire using a reference electrode located 1/2 in. below the cathode. The reference electrode reveals that about 75 percent of the voltage
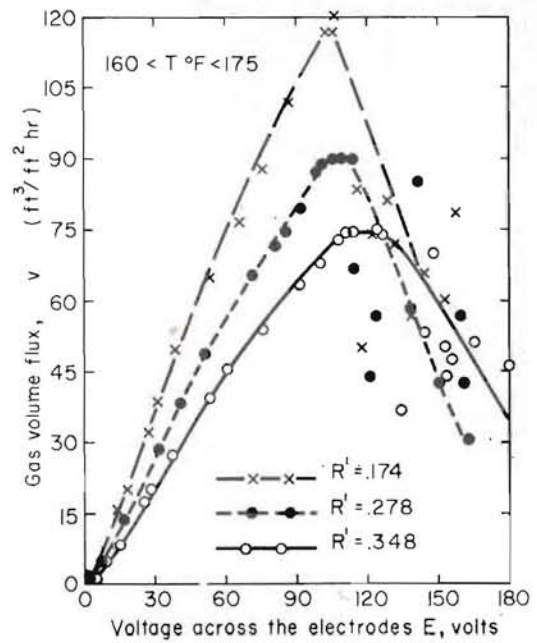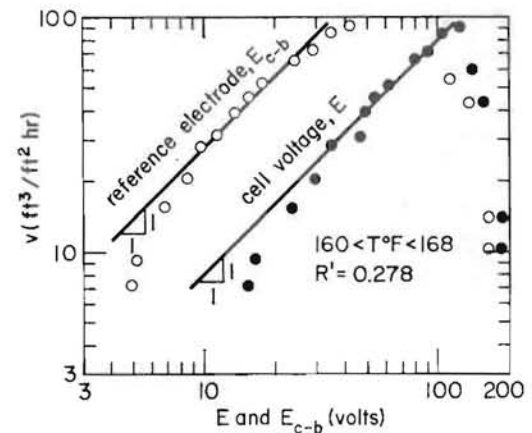
drop is being sustained across the cell, away from the cathode. The actual surface voltage drop would be still substantially less than that measured on the reference electrode.

Our system was therefore one in which the current varied almost entirely by virtue of changes in potential across the cathode, the remaining resistance being constant. The curves accordingly should have the right shape although the abscissas are arbitrary within a constant factor.

An additional source of error in the system is the possible contribution of vapor generation. Since this could hardly have been a significant factor before the onset of sparking and corona, and since sparking only occurred once the peak had been reached, its contribution to our observations of the peak could not have been great. However a second source of error is compensatory and comparable in magnitude. This is the fact that "current yield" efficiencies can run below 100 percent (see, *e.g.*, [23]) so that Faraday's law might underestimate the hydrogen gas yield by a few percent. These effects probably give a net error somewhere between 0–10 percent. At voltages beyond the peak there might be considerable vapor generation. Probably the film electrolysis regime is, in fact, a mixed boiling and electrolysis
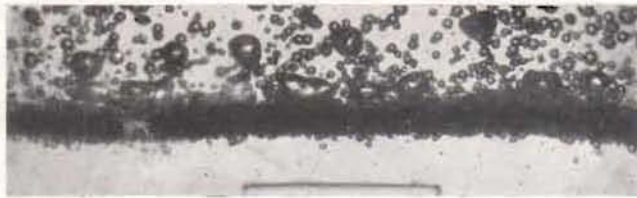
$v = 82.3$ ft^3/ft^{2}hr, $E = 95$ volts
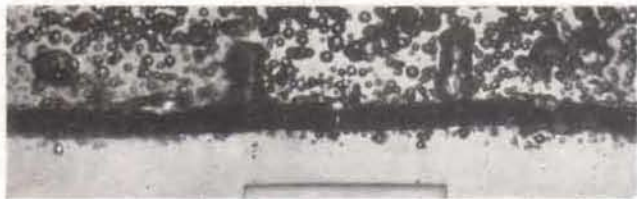
$v = 82.3$ ft^3/ft^{2}hr, $E = 97$ volts
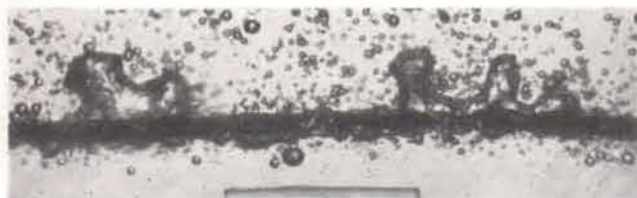
$v = 87.3$ ft^3/ft^{2}hr, $E = 108$ volts

$v = 28.9$ ft^3/ft^{2}hr, $E = 168$ volts
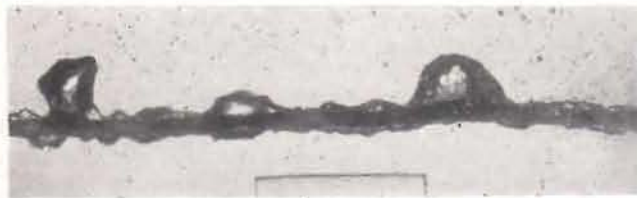
$v = 24.8$ ft^3/ft^{2}hr, $E = 173$ volts

$v = 33.0$ ft^3/ft^{2}hr, $E = 176$ volts

Fig. 6 Photographs of electrolysis in a 0.1 normal KOH solution on a 16-gauge ($R' = 0.278$) wire

Table 1 Observed heat flux at first transition in boiling

Radius (inches)	Water			Methanol	
	R'	$(\rho_g h_{fg}) v_{sc}$ 10^4Btu/ft^{2}hr		R'	$(\rho_g h_{fg}) v_{sc}$ 10^4Btu/ft^{2}hr
.0160	.174	$8.14 {}^{+.50}_{-.49}$		.258	$4.41 {}^{+.06}_{-.06}$
.0200	.218	$4.30 {}^{+.08}_{-.09}$		.323	$3.03 {}^{+.08}_{-.08}$
.0255	.278	$4.57 {}^{+.05}_{-.05}$		.412	$2.08 {}^{+.07}_{-.08}$
.0320	.348	$2.61 {}^{+.10}_{-.10}$		.516	$.98 {}^{+.03}_{-.02}$

region owing to the greatly increased surface resistance at the cathode and the resulting heat generation.

The results of the tests as plotted in Figs. 4 and 5 verify the essential linearity of current (or v) in voltage, after nucleate electrolysis becomes fully established. This linearity is established only after a layer of bubbles has been established to preclude microconvection.

Fig. 6 is a sequence of pictures of electrolysis on the 16-gauge wire ($R' = 0.278$) beginning slightly below the maximum current and continuing to $E = 176$ volts. The 1.1 cm (0.433 in.) wide marker is evident at the bottom of each picture. The corona and sparking are invisible in these pictures, back-illuminated with a high-intensity stroboscope. The slugs and columns are very clear on the wire in the first two pictures. As E is increased these jets appear to give way to a film process characterized by Taylor unstable waves very similar to these observed during pure film boiling (see, e.g. [15 or 25]).

The second experiment used Sun's [12] apparatus to observe q at the first transition on horizontal wires during boiling in methanol and water. Since the apparatus and basic procedure do not differ from that described in [12] we shall not reproduce details here. In this case we observed the first transition with the help of a stroboscope and checked our visual impressions with still photographs.

Table 1 lists the observed transition points for the two liquids and for the four wire sizes. We were generally able to identify the transitions reproducibly within a 6 percent margin, but only after identifying a particular stage (within a broader transition range) in which the first few jets appeared to take form.

Discussion of Results

We now have the following claims as to the character of electrolysis, and data against which to test them:

Microconvection Does Not Abet Current (or Volume) Flux in Electrolysis. A corollary of this claim was that, in the nucleate electrolysis regime, I or v should be approximately linear in E (or E_{e-b}) up to the point of hydrodynamic transition. Figs. 4 and 5 clearly bear this out very well, as did Kellogg's experiment. Given this to be true we then expect that

The Volume Flux Maximizes at the First Transition, Instead of the Second, in Electrolysis. Four kinds of evidence bear this out. The first is the lack of microconvective enhancement of I. The second is the visual appearance of the process, Fig. 6, which matches the appearance of the first transition in boiling.

The third piece of evidence arises from the fact that equation (5) predicts v_{max} in the range from 32,000 to 39,000 ft^3/ft^{2}hr for our test wires. Thus v_{max} is predicted to be between 270–520 times the observed maximum, depending upon the wire size. It follows that the maximum could not possibly reflect the second transition. The reader who is acquainted with boiling might justly wonder how this ratio could reasonably be so high. The

Table 2 Measured contact angles

Liquid and metal	Source	Temp. (°F)	β range (degrees)
water-stainless steel	[26]	86	38-78
water-stainless steel	[26]	212	28-82
$\frac{1}{10}$ N, KOH - platinum*	[27]	74	15-35
$\frac{1}{10}$ N, KOH - nichrome wire*	[28]	74	10-23
water - copper	[29]	212	60
methanol - copper	[29]	147	46
water - nichrome	present	81	60-81
methanol - nichrome	present	81	40-52

*data for electrolytic H_2 bubbles in situ.

reason is that for either cylinders or flat plates the ratio of transition volume fluxes is

$$\frac{v_{sc}}{v_{max}} \simeq f(\beta, R') \sqrt{\frac{\rho_g}{\rho_f}} \qquad (16)$$

Since ρ_g is extremely small for H_2 the ratio is quite small. The same would be true for boiling at low pressure.

The fourth piece of evidence lies in our third claim; namely,

Equation (15) Describes the First Transition in Both Boiling and Electrolysis. To apply equation (15) one must first ascertain the contact angle, β, for water, methanol, and tenth-normal KOH electrolyte, since $v_{sc} \sim \beta^{3/2}$. Unfortunately β is a notoriously stochastic property. In 1959 Griffith and Wallis [26] pointed out the difficulty of reproducing β consistently. Table 2 shows the great variability of their data with slight changes of surface condition. Trivedi and Funk [27] provided in situ measurements of contact angles under static bubbles during electrolysis in normal KOH electrolyte on platinum plates. Trivedi [28] recently measured β during electrolysis in tenth-normal KOH on nichrome wires. The data of [26 and 27] are included in Table 2. Both sets of data were obtained on metals that had been first cleaned in distilled water, then in methanol, and finally rinsed in the test liquid. Chang and Snyder [29] also reported values for methanol and water which they inferred from the data of earlier papers. These values are included in Table 2.

Table 2 also includes original β-values that we measured using the tilting plate method[6] for methanol and the sessile drop method[6] for water. Both tests used nichrome plates cleaned in the same way that Trivedi's surfaces were.

The four measured values of v_{sc} in electrolysis (the peaks in Figs. 4 and 5) and the eight values of v_{sc} for boiling are given in Fig. 7. They are nondimensionalized as $v_{sc}/\beta^{3/2} \sqrt[4]{g\sigma(\rho_f - \rho_g)}$ and plotted against $1/R'$, since equation (15) indicates that this group should equal $0.0001464/C_3 R'$. The observed values of v_{sc} are spread out considerably in this representation owing to our ignorance of precise values of β. For the boiling results we used our own measurements of β and for the electrolysis data we used Trivedi's values of β for electrolysis on nichrome wires.

Fig. 7 shows that the $1/R'$ dependence of v_{sc} is upheld, although the slopes differ between water and methanol. The water data for both electrolysis and boiling are fairly well represented with equation (15) if C_3 is taken to be 4.4. This value of C_3 corresponds nicely with the proportioning of the jets that we observe in the first two pictures in Fig. 6 (taken near the point of maximum v). A value of C_3 more nearly equal to 2.5 would be required to represent the methanol data in Fig. 7.

As E Is Increased Beyond the Point of Peak Volume Flux, the Process Goes to a Kind of Film Process Similar to Film Boiling. The photographs in Fig. 6 show an evolution from gas removal by slugs

[6] A detailed explanation of such tests is given in reference [26].
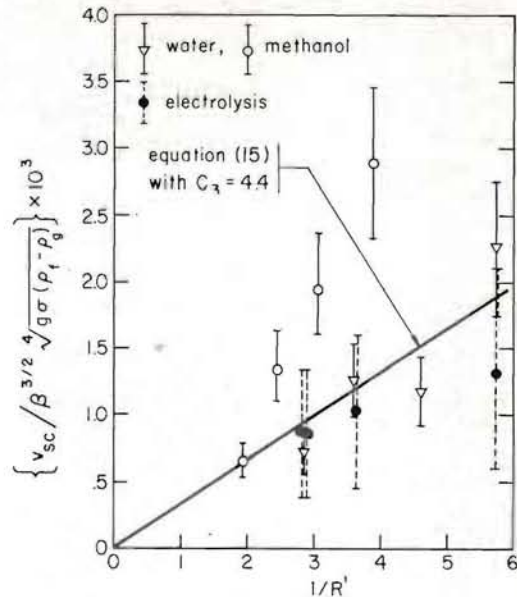
Fig. 7 Comparison of predicted first transition with data for both boiling and electrolysis

and columns, to gas-vapor removal by the cyclic collapse of Taylor unstable waves. The wavelengths measured from the last three photographs in Fig. 6 and from other pictures not included here are

$$(\lambda_d)_{experimental} = 0.42 \pm 0.10 \text{ in.}$$

while equation (9) gives $\lambda_d = 0.41$ in.

The wire appears to become almost completely blanketed in the pictures for high voltages. However, a small number of departing nucleation bubbles in the pictures suggests that there is still some liquid-to-cathode contact. Despite these indications of a conventional approach to a film-gas removal process, there is a difficulty in the numerical value of v_{min}. Equation (10), which (as we have noted) might overestimate v_{min}, gives

$$v_{min}(R' = 0.174) = 149 \text{ ft}^3/\text{ft}^2\text{hr}$$

$$v_{min}(R' = 0.348) = 99 \text{ ft}^3/\text{ft}^2\text{hr}$$

while the corresponding experimental values of v_{sc} are 120 and 75, respectively.

Thus $v_{sc} < v_{min}$, and beyond $E(v_{sc})$ the calculated volume flux of H_2 drops still farther below v_{min}. This is additional evidence that stable film electrolysis involves a substantial component of evaporated water which does not appear in the v_{sc} calculation based on Faraday's law.

Conclusions

1 There is an enhancement of heat transfer which occurs in boiling when nucleation sites influence one another; this does not occur in electrolysis. Consequently $v \sim E$ in the region below the first transition.

2 The volume flux reaches a local maximum at the "first transition" point, or the transition from isolated bubbles to slugs and columns.

3 The volume flux, v_{sc}, at the first transition on small horizontal cylinders is given approximately by equation (15). However, our ignorance of precise values of β and of the precise structure of the escaping gas jets precludes accuracy beyond a factor of two in the use of equation (15). The predicted dependence of v_{sc} on $1/R'$ appears to be sound.

4 A form of electrolysis that shows many outward appear-

ances of film boiling, including the Taylor unstable wavelength, are established at high voltage.

5 A clear understanding of transitional and film electrolysis and an identification of v_{min} in electrolysis must await experimentation in a system with an extremely high voltage capability and a substantial cell cooling system.

6 The existing body of understanding of boiling processes provides a very useful point of departure for seeking to extend our understanding of gas-forming electrolysis.

References

1 Wydeven, T., and Jonson, R. W., "Water Electrolysis: Prospects for the Future," *Journal of Engineering for Industry*, TRANS. ASME, Series B, Vol. 90, 1968, p. 531.

2 Secord, T. C., and Ingelfinger, A. L., "Life Support for Large Space Stations," *Astronautics and Aeronautics*, Feb. 1970, p. 56.

3 Bhattacharya, A., and Lienhard, J. H., "Similarity of Vapor and Gas Bubble Growth," *Iranian Journal of Science and Technology*, Vol. 1, No. 2, 1971, pp. 113–129.

4 Zuber, N., "Hydrodynamic Aspects of Nucleate Pool Boiling—Part I," Report No. RW-RL-164, Ramo Wooldridge Research Laboratory, Conoga Park, Calif., Jan. 1960.

5 Zuber, N., "Nucleate Boiling. The Region of Isolated Bubbles and the Similarity With Natural Convection," *International Journal of Heat and Mass Transfer*, Vol. 6, 1963, pp. 53–78.

6 Moissis, R., and Berenson, P. J., "On the Hydrodynamic Transition in Nucleate Boiling," *Journal of Heat Transfer*, TRANS. ASME, Series C, Vol. 85, No. 3, 1963, pp. 221–229.

7 Moissis, R., and Griffith, P., "Entrance Effects in a Two-Phase Slug Flow," *Journal of Heat Transfer*, TRANS. ASME, Series C, Vol. 84, 1962, pp. 29–39.

8 Griffith, P., and Wallis, G., "Slug Flow," M.I.T. Division of Spons. Research, Report No. 15, Project 7-7673, 1959.

9 Zuber, N., "Hydrodynamic Aspects of Boiling Heat Transfer," AEC Report No. AECU 4439, *Physics and Mathematics*, 1959.

10 Zuber, N., Tribus, M., and Westwater, J. W., "The Hydrodynamic Crisis in Pool Boiling in Saturated and Subcooled Liquids," *International Developments in Heat Transfer*, No. 27, ASME, New York, 1963, pp. 230–236.

11 Bellman, R., and Pennington, R. H., "Effects of Surface Tension and Viscosity on Taylor Instability," *Quarterly of Applied Mathematics*, Vol. 12, 1954, p. 151.

12 Sun, K. H., and Lienhard, J. H., "The Peak Pool Boiling Heat Flux on Horizontal Cylinders," *International Journal of Heat and Mass Transfer*, Vol. 13, 1970, pp. 1425–1439.

13 Ded, J. S., and Lienhard, J. H., "The Peak Pool Boiling Heat Flux from a Sphere," to appear in *A.I.Ch.E. Journal*.

14 Berenson, P. J., "Transition Boiling Heat Transfer From a Horizontal Surface," M.I.T. Heat Transfer Laboratory Technical Report No. 17, 1960.

15 Lienhard, J. H., and Wong, P. T. Y., "The Dominant Unstable Wavelength and Minimum Heat Flux During Film Boiling on a Horizontal Cylinder," *Journal of Heat Transfer*, TRANS. ASME, Vol. 86, No. 2, Series C, 1964, pp. 220–226.

16 Kovalev, S. A., "An Investigation of Minimum Heat Fluxes in Pool Boiling of Water," *International Journal of Heat and Mass Transfer*, Vol. 9, 1966, p. 1219.

17 Lienhard, J. H., "Interacting Effects of Gravity and Size Upon the Peak and Minimum Boiling Heat Fluxes," NASA CR-1551, May 1970.

18 Tien, C. L., "A Hydrodynamic Model for Nucleate Pool Boiling," *International Journal of Heat and Mass Transfer*, Vol. 5, 1962, p. 533.

19 Boehm, R. F., and Lienhard, J. H., "Transient Effects in Tien's Nucleate Boiling Model," ASME Paper No. 64-WA/HT-34.

20 Kirby, D. B., and Westwater, J. W., "Bubble and Vapor Behavior on a Heated Horizontal Plate During Pool Boiling Near Burnout," *Chemical Engineering Progress*, Vol. 61, No. 57, 1965, pp. 238–248.

21 Jakob, M., *Heat Transfer*, Vol. 1, Wiley, New York, 1955, p. 630.

22 Kellogg, H. H., "Anode Effect in Aqueous Electrolysis," *Journal of Electrochemical Society*, Vol. 97, 1950, pp. 133–142.

23 Meyer, R. E., "Faraday's Laws," *Encyclopedia of Electrochemistry*, Hampel, C. A., ed., Reinhold Publishing Co., 1964, pp. 592–594.

24 Bhattacharya, A., "The Analogy Between Gas Removal Processes in Boiling and Electrolysis," University of Kentucky, College of Engineering, Technical Report UKY 35-71-ME10, July 1971.

25 Lienhard, J. H., and Sun, K. H., "Effects of Gravity and Size Upon Film Boiling From Horizontal Cylinders," *Journal of Heat Transfer*, TRANS. ASME, Series C, Vol. 92, No. 2, 1970, pp. 292–298.

26 Griffith, P., and Wallis, J. D., "The Role of Surface Conditions in Nucleate Boiling," *Chemical Engineering Symposium Series*, Storrs, Conn., No. 30, Vol. 56, 1960, pp. 49–63.

27 Trivedi, G., and Funk, J. E., "Dynamics and Stability of Electrolytic Bubbles: Bubble Departure Diameters," University of Kentucky, College of Engineering, Technical Report UKY 28-70-MES, 1970.

28 Trivedi, G., unpublished results, University of Kentucky Boiling and Phase-Change Laboratory, 1971.

29 Chang, Y. P., and Snyder, N. W., "Heat Transfer in Saturated Boiling," *Chemical Engineering Symposium Series*, Storrs, Conn., No. 30, Vol. 56, 1960, pp. 25–38.